Research paper

Active control of superposition of waves with time lagging and frequency difference: Numerical simulation

Y. M. Kong[a] and W. Y. Tey[a, b*]

aDepartment of Mechanical Engineering, Faculty of Engineering, Technology, and Built Environment, UCSI University, Cheras 56000 Kuala Lumpur, Malaysia
bMalaysia-Japan International Institute of Technology, Universiti Teknologi Malaysia Kuala Lumpur, 54100 Kuala Lumpur, Malaysia

Abstract

The theory of superposition of waves has been widely deployed in many engineering applications such as medical imaging, engineering measurements, and wave propagation in structures. However, these applications are prone to the interference of unwanted waves. The root cause of the weakness could be ascribable to the wave propagation pattern, which is not actively controlled. A new concept of imposing a time-lagging effect on the source of the wave as an active wave emission strategy is introduced and discussed in this paper. A numerical solver has been developed based on the finite volume Euler explicit method to investigate the wave propagation pattern when there is a time-lagged effect and frequency difference at the source of the wave. Our results reveal that time-lagged wave propagation will be more immune to the disturbance of other waves. The larger the time lag, the more resilient the wave is to resist the interference of other waves, even at a higher frequency. Time-lagged waves can be regarded as a promising active wave emission method that has many potential and robust engineering applications to be explored in the future.

1. Introduction

Wave is a physical phenomenon in which the medium particles experience compression and rarefaction alternatively to transfer energy from one end to another. Indeed, the physics of waves has been widely applied in various engineering applications. For instance, ocean wave energy can be harnessed using various converting technologies [1-4], and it is indeed one of the hottest renewable energies being investigated to replace conventional fossil energy. With the omnipresent applications of electrical appliances, the electromagnetic wave emission from these devices may give rise to the

menacing health issue. Great attention has been given recently to the absorption and shielding technology of electromagnetic waves [5-8]. Moreover, ultrasonic wave propagation has been a popular method being widely applied for various detection purposes, including welding spots, military surveillance, and engineering fatigue crack sensing [9,10]. Ultrasonic wave irradiation may induce the cavitation of bubbles, which can lead to applications such as coal aggregation [11], separation of emulsion [12,13], treatment of radioactively affected wastewater [14], and ultrasonic pretreatment on biomass [15,16]. Thermo-acoustical devices for heat generation are also designed using the physics of wave propagation [17,18]. Recently, structural vibration is also studied based on elastic wave propagation [19-22]. Doppler's effect [23,24], due to moving wave sources, also remains an interesting topic in biomedical and military applications. Although extensive research has been done, these applications are limited to single-source waves without actively manipulating the propagation pattern. These emissions transpire in a smooth and continuous sinusoidal pattern, without regular, conscious, and purposeful straggling for the next wave cycle.

In the real physical world, there is always more than one wave source that might co-exist, and their interactions will create a complex wave phenomenon. Such interaction is named superposition, in which its alternative constructive and destructive interference from coinciding independent waves will complicate the problem. Therefore, the investigation of trailed superposition of waves is required to enable active wave pattern control for various potential applications. The possible applications may comprise the improvement of cavitation in the ultrasonic process, the destruction of the unwanted wave, or the propagation of a wave that is more immune to the disturbance of another wave.

There are very limited studies on the superposition of waves. For example, Nicassio et al. [25] and Yu et al. [26] investigated the effect of wave interference on the material structure. Some preliminary applications of wave interference were reported in the prediction of the dye absorption process [27], displacement measurement [28], measurement of lubricant film thickness [29], and ultrasonic pretreatment [30]. Nonetheless, these works do not demonstrate proactive control of wave superposition, which would hinder more sophisticated engineering applications.

Hence, the objective of the paper is to investigate the wave propagation effect with an active control on the time-lagging wave source with varied frequency differences. A solver which enables the active frequency difference and time-lagging control was developed in the current work. The interference due to different radiation modes (radial-radial and radial planar wave emission) is discussed in the paper. The current work renders an introduction to a new strategy of wave emission: trailed propagation. The proposed wave motion is novel as it is more immune to the disturbance and superposition from other waves.

2. Numerical solution and design of the algorithm

2.1. Euler explicit method for wave equation

Consider the two-dimensional wave equation as in Eq. (1):

$$\frac{\partial^2 P}{\partial t^2} = c^2 \left(\frac{\partial^2 P}{\partial x^2} + \frac{\partial^2 P}{\partial y^2} \right) \tag{1}$$

where P, t, c, x, and y are the local scalar field displacement, time, wave's speed, x-component, and y-component spatial domain, respectively. Discretisation on Eq. (1) using the Euler explicit method [31] will form Eqs. (2.1-2.3):

$$\frac{\partial^2 P}{\partial t^2} = \frac{P_{i,j}^{n+1} - 2P_{i,j}^n + P_{i,j}^{n-1}}{\Delta t^2} \tag{2.1}$$

$$\frac{\partial^2 P}{\partial x^2} = \frac{P_{i+1,j}^n - 2P_{i,j}^n + P_{i-1,j}^n}{\Delta x^2} \tag{2.2}$$

$$\frac{\partial^2 P}{\partial y^2} = \frac{P_{i,j+1}^n - 2P_{i,j}^n + P_{i,j-1}^n}{\Delta y^2} \tag{2.3}$$

where Δt, Δx and Δy are the time step, grid size in the x-component, and y-component domains, respectively. By taking $\Delta x = \Delta y$, the equation can finally be rearranged to form Eq. (3). Eq. (3) will be used to solve the wave simulation, where multiple iterations will be performed using MATLAB to find the solution:

$$P_{i,j}^{n+1} = -P_{i,j}^{n-1} + 2P_{i,j}^n + \zeta \chi^n_{i,j} \tag{3}$$

where

$$\chi^n_{i,j} = P_{i+1,j}^n + P_{i-1,j}^n + P_{i,j+1}^{n+1} + P_{i,j-1}^{n-1} - 4P_{i,j}^n \tag{4}$$

$$\zeta = c^2 \frac{\Delta t^2}{\Delta x^2} \tag{5}$$

The explicit solution as in Eqs. (3) – (5) requires the storage of three sets of variables: the previous wave information, the current wave information, and the future wave information. Upon the analysis, the future wave will be the new current wave, while the old current wave will then be set to become the new previous wave. The process keeps iterating until a predefined time limit command is fulfilled.

Next, to fulfill the Courant-Friedrichs-Lewy (CFL) condition [32], where the CFL number is equivalent to the square root of ζ, the relationship between time step Δt, and spatial distance Δx as in Eq. (5) will be calculated. CFL condition is important to ensure stable time marching, regardless of the first-order parabolic equation or the second-order hyperbolic equation [31,32]. It defines the ratio between the time step and grid size, i.e., a smaller time step shall be implemented with a higher resolution of spatial discretised distance. Most of the time, CFL shall not go beyond 1.0. A CFL of 0.5 is applied for the current study, and results show a stable time marching without numerical noise.

2.2. Time-lagging algorithm

To produce time lagging between each wave pulse, the time lagging coefficient must first be defined. Time lagging can be defined as the time pause between each period of the wave. The frequency from each wave source will be fixed at the start of the simulation. Therefore, the frequency of the wave is given as a constant represented by frequency, f. With the new constant f, time can be redefined using the relation between period and time by including the time lagging coefficient, α, as Eq. (6).

$$f = \frac{\alpha}{t} \rightarrow \alpha = ft \tag{6}$$

Now the relationship between lagged time t_{lag} and frequency f can be described using Eq. (7):

$$t_{lag} = \frac{\alpha}{f} \tag{7}$$

From Eq. (7), the time lag of the wave can be controlled by manipulating α. For instance, when α

= 1, there will be a time lag equivalent to the amount of time taken for the wave to complete one oscillation between each oscillation of a wave. Let the lag time of a wave t_{lag} as shown in Eq. (7), be t_2, and the period of the wave be t_1. The total time passed at any given moment can then be defined as T_n. T_n can then be defined using t_1 and t_2 as in Eq. (8).

$$T_n = at_1 + bt_2 + C \tag{8}$$

The constant C is the amount of time remaining after subtracting 'a' amount of t_1 and 'b' amount of t_2 from the total time T_n. The equation will then be rearranged to form the following:

$$C = T_n - (at_1 + bt_2) \tag{9}$$

To solve the algorithm, let $a = b$. It can be assumed that there is an equal amount of a and b at the given time T_n. In any situation, there can only be two scenarios, $a = b$ or $a = b + 1$. In the current algorithm, $a = b$ is applied. The new equation will then be defined as shown in Eq. (10).
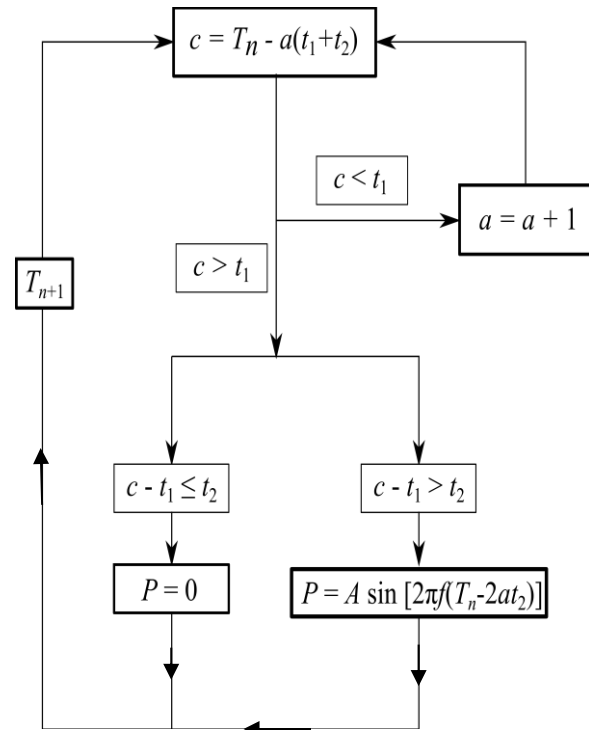
$$C = T_n - a(t_1 + t_2) \tag{10}$$

Fig. 1. The logic flow of the time-lagging algorithm.

The steps discussed above can be represented via Fig. 1. Using the flow chart as shown in Fig. 1, a wave source can then be produced as shown in Fig. 2. Note that there will be a zero-amplitude after and before one cycle of the wave. Therefore, combining the time-lagging algorithm and finite differencing scheme could effectively generate wavefront with time retention.
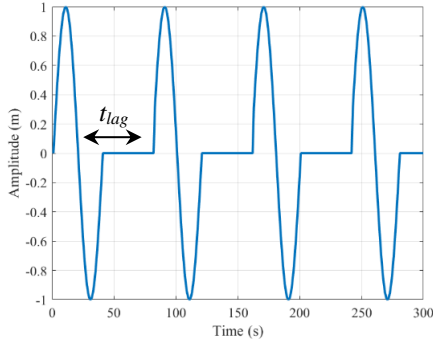

Fig. 2. Time lagged wave source produced.

2.3. Numerical details and physical modeling

We developed an in-house code using the principle discussed above, and multiple variables can be manipulated. In this study, the chosen controlled variable is the frequency difference, time-lagging coefficient, and the pattern of wave superposition. Two types of superposition will be investigated: superposition between radial-and-radial wave propagation and planar-and-radial wave propagation.

The research domain is shown in Table 1. The location and the amplitude of the superposed wave will be the parameters of interest to be captured.

Table 1. Variables involved in the design of the numerical investigation.

α	0.0	0.5	1.0
Radial-radial case	(a) $\Delta f = 0$ (b) $\Delta f \neq 0$	(a) $\Delta f = 0$ (b) $\Delta f \neq 0$	(a) $\Delta f = 0$ (b) $\Delta f \neq 0$
Radial-planar case	(a) $\Delta f = 0$ (b) $\Delta f \neq 0$	(a) $\Delta f = 0$ (b) $\Delta f \neq 0$	(a) $\Delta f = 0$ (b) $\Delta f \neq 0$

In the current work, the grid size of 800×800 is applied on a square domain of 8 m $\times$ 8 m. The instantaneous wave amplitude for the source of wave can be described as in Eq. (11). The speed of wave c is set as 1 m/s. Meanwhile, at the wall far away from the source of the wave, the absorbing boundary condition is applied. In other words, we simulated a condition where the wave is freely propagated without interference due to wall reflection. The boundary condition can be imposed using the Neumann boundary condition, as shown in Eq. (12). Eq. (12) is then further developed from Eqs. (13.1) – (13.4) represents the boundary condition at the left side, right side, top side, and bottom side of the square shape problem domain.

$$P_{source} = A\sin\left(2\pi f t\right) \tag{11}$$

$$\frac{\partial}{\partial x}\left(\frac{\partial^2 P}{\partial t^2}\right) = 0 \tag{12}$$

$$P_{i,1}^{\,n+1} = P_{i,2}^{\,n-1} \tag{13.1}$$

$$P_{m,1}^{\,n+1} = P_{i,m-1}^{\,n-1} \tag{13.2}$$

$$P_{1,j}^{\,n+1} = P_{2,j}^{\,n-1} \tag{13.3}$$

$$P_{k,j}^{\,n+1} = P_{k-1,j}^{\,n-1} \tag{13.4}$$

The subscript of n, m, and k is the time step, maximum x-component grid, and maximum y-component grid, respectively. A is the maximum amplitude of the wave.

3. Results and discussion
3.1. Verification of results

Only one-dimensional cases will be studied during the verification stage, and thus Eq. (3) can be reduced to Eq. (14).

$$P_i^{n+1} = -P_i^{n-1} + 2P_i^n + \zeta(P_{i+1}^n - 2P_i^n + P_{i-1}^n) \tag{14}$$

The results of the one-dimensional wave without time-lagged are shown in Fig. 3. The result is computed by setting $f = 1$ Hz, $A = 1$ m while $c = 1$ m/s. From the figure, the wavelength λ is 1 m, the same as the value calculated from a simple theory equation as shown in Eq. (15).

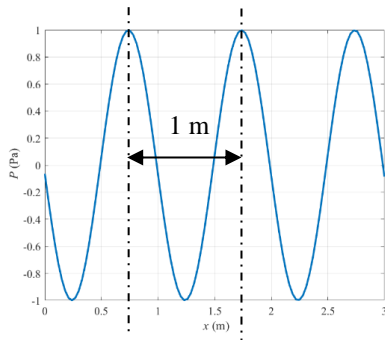$$c = f\lambda \rightarrow \lambda = c / f \tag{15}$$

Fig. 3. One-dimensional wave propagation without time-lagged generation of wave source.

3.2. Radial-radial superposition of wave

The sources of radial waves are in a colinear line, placed at the horizontal middle line of the problem domain. In this section, all the wave parameters taken are the same as in the previous section, but with a total time of 7.2 seconds. The produced wave pattern due to frequency difference and time-lagging effect can be shown in Figs. 4-6. For all the figures in this subsection, the wave source at the right-hand side is the only source being manipulated (i.e., with higher f and α).
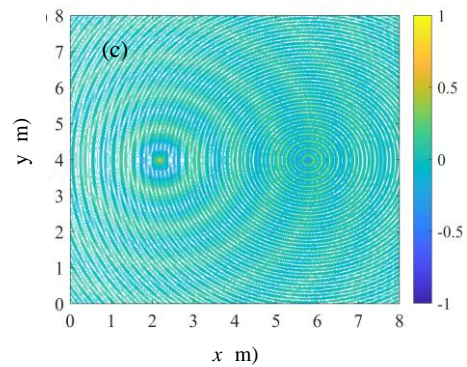

Fig. 4. Superposition of wave at $\alpha = 0$ (without time-lagging effect) when the frequency difference is: (a) 0 Hz, (b) 2 Hz, and (c) 4 Hz.
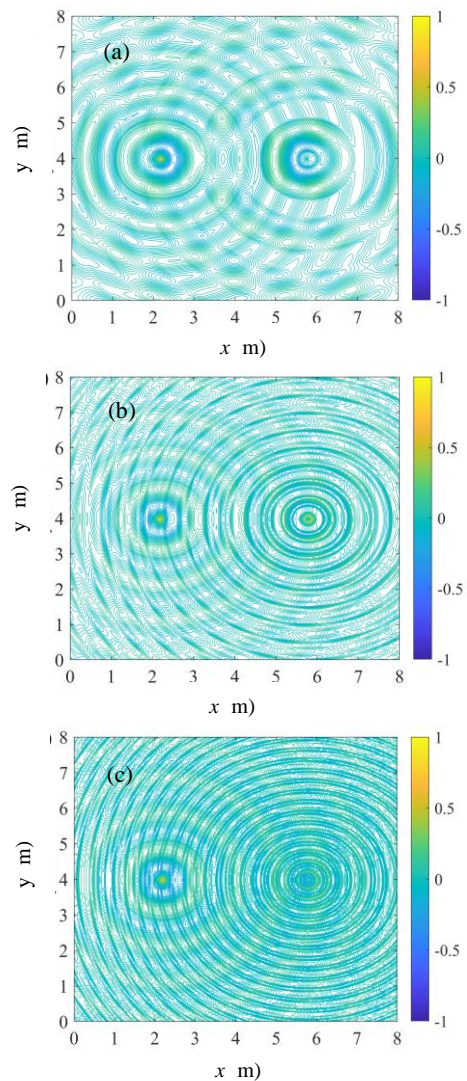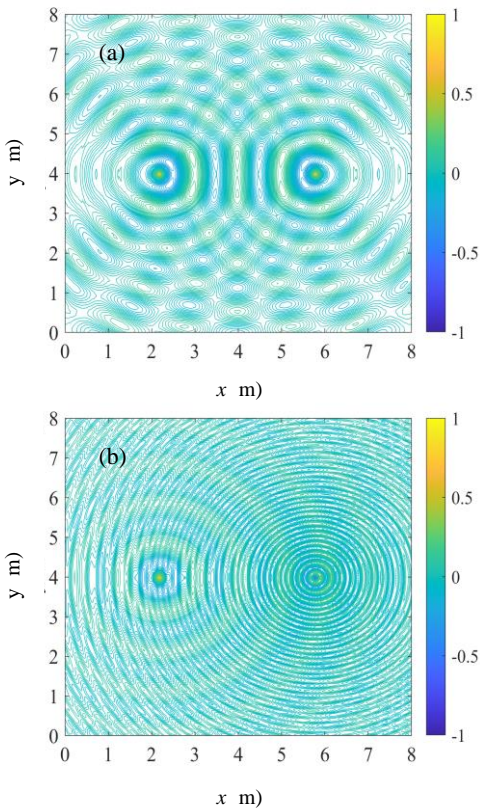

Fig. 5. Superposition of wave at $\alpha = 0.5$ (with time-lagging effect) when the frequency difference is: (a) 0 Hz, (b) 2 Hz, and (c) 4 Hz.

Based on Figs. 4-6, when both waves are emitting with the same frequency, the constructive-destructive superposition line for both sources is indeed a straight line and equally distributed over the source of the wave. However, when the frequency of one of the sources (right-hand-side source) is increased, the source with a lower frequency will start to dominate the wave propagation. The constructive-destructive superposition line of the source with higher frequency will be deflected into a parabolic curve towards the lower-frequency source.

When the frequency difference becomes larger (i.e. 4 Hz), the lower frequency source will completely dominate the propagation, almost removing the propagating effect of the source with high frequency. Its difference from solo-source wave propagation is that every ripple of wave propagation is now associated with many tiny wave undulations along the ripple radius.

If the frequency of sources is different, the general wave propagation will be dominated by the source with a lower frequency. However, when the time-lagging effect of the source is included, the parabolic constructive-destructive superposition line would disappear. Therefore it can be observed that the time delay has compensated for the deviation of the parabolic constructive-destructive superposition line.

With the discovery as discussed above, in the future, if one needs to maintain the constructive-destructive superposition line without interference from other waves with different frequencies, the control of the time delay could be a good strategy. The potential applications can be extended into the state-of-the-art quantum-mechanical system [33], which comprises the precise control of electromagnetic wave [34], particle diffusion [35], and the discovery of cosmos waves [36].

3.3 Radial-radial superposition of wave

Since planar wave propagation would take a long time across the 8 m length of the domain, for radial-planar wave propagation, the time set is 20 seconds to enable complete wave propagation and interference. The frequency and time-lagging effect of the planar wave source are manipulated. Fig. 7 shows the interference between a radial wave and a planar wave without time lagging. A similar range

of frequency difference between the wave source as described in the previous section is applied.

In a condition where the radial wave and the planar wave have a similar frequency, the wave propagation follows the planar wave propagation style. The amplitude of the planar wave remains high without any "attenuation" due to its preserved propagated area for the next wavelet. In radial wave, in contrast, the wave amplitude will become smaller as it moves away from the source.
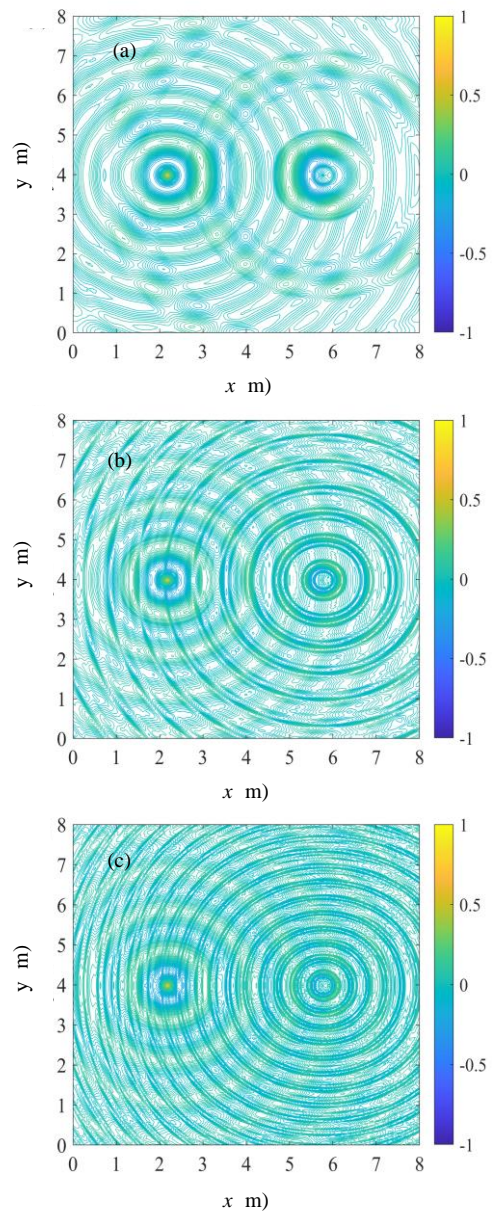

Fig. 6. Superposition of wave at $\alpha = 1.0$ (with time-lagging effect) when the frequency difference is: (a) 0 Hz, (b) 2 Hz, and (c) 4 Hz.
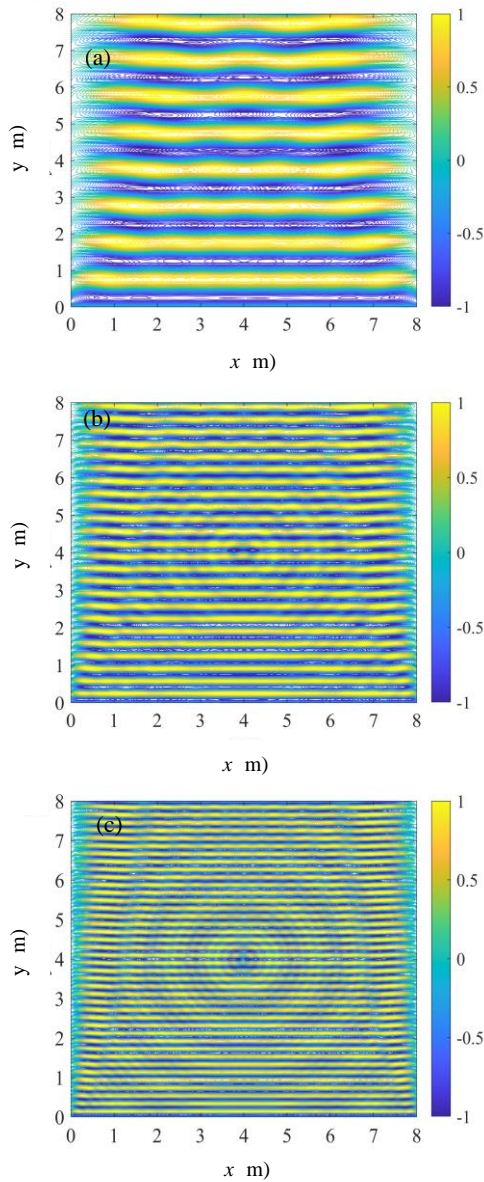
Fig. 7. Superposition of wave at $\alpha = 0$ (without time-lagging effect) when the frequency difference is: (a) 0 Hz, (b) 2 Hz, and (c) 4 Hz, with the planar wave to be the wave with higher frequency.

The enlarging of the propagated area for the next wavelet has reduced the wave intensity and energy. With decreasing wave power, the amplitude of the wave will be reduced. Eq. (16) relates the intensity I and the wave power W:

$$I = \frac{W}{4\pi r^2} \tag{16}$$

Where r is the radial distance from the source of noise [37].

As from Fig. 7(a), only the planar wave near the source of the radial wave is slighted and sliced into a few sections. The planar wave is reattached again after some distance away from the source of the radial wave. However, from Fig. 7-9, it can be observed again that the low-frequency source is the dominator of the wave pattern. A high-frequency source will act more like a splitter for low-frequency wave ripples.
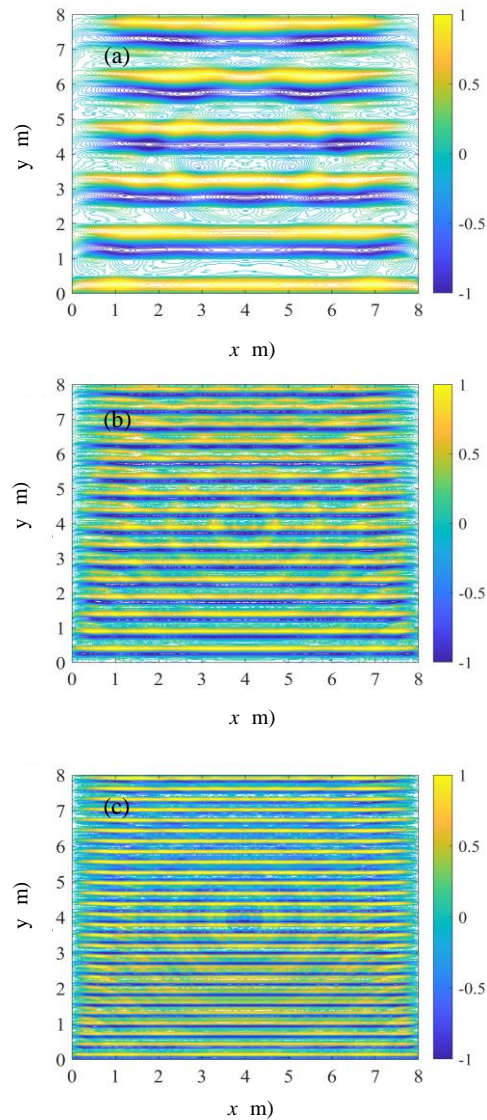

Fig. 8. Superposition of wave at $\alpha = 0.5$ (with time-lagging effect) when the frequency difference is: (a) 0 Hz, (b) 2 Hz, and (c) 4 Hz, with the planar wave to be the wave with higher frequency.

On the other hand, waves with different frequency sources appear to have a curving pattern for their constructive and deconstructive line. Similarly, the pattern is consistent throughout all lagging coefficients, while the constructive interference points have equal amplitude throughout all α.

For the planar-radial superposition of waves, it could be observed that when the planar wave interferes with the radial wave, the deconstructive interference will break apart the straight planar waves. Both frequency and lagging coefficient will affect the breakage pattern differently.
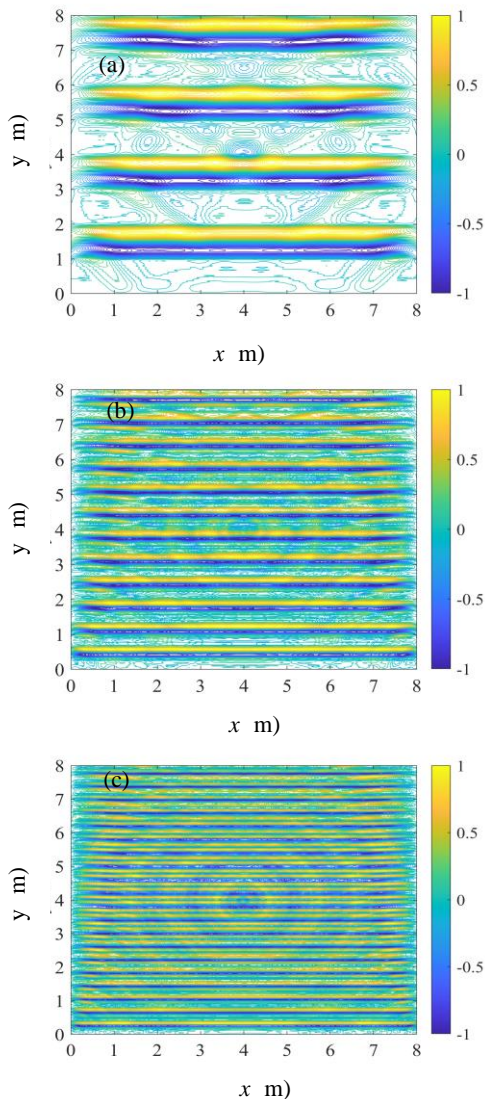

Fig. 9. Superposition of wave at $\alpha = 1.0$ (with time-lagging effect) when the frequency difference is: (a) 0 Hz, (b) 2 Hz, and (c) 4 Hz, with the planar wave to be the wave with higher frequency.

4. Conclusions

The difference between the superposition of each wave has been produced and compared. The comparison has shown that although each interference pattern is different, multiple similarities can be identified. Radial-radial superposition shares a consistent line of constructive and destructive interference, while planar-radial superposition has shown that a certain pattern could be produced by manipulating frequency and time-lagging coefficient.

As the concluding remarks, the main findings of the active control on the superposition of wave via time lagging and frequency difference can be summarised into the following points.

- For the case without time delay of the source of wave, the low-frequency wave will deviate from the constructive-destructive superposition line of the high-frequency wave. With a high-frequency difference, the lower-frequency wave will command wave propagation while the high-frequency wave will act as the wave splitter.

- If the low-frequency radial wave has almost similar acoustic energy to the planar wave, the ripples of the planar wave will be partitioned into several subsections, regardless of the existence of the time-lagged effect and vice versa. The "partitioning" wave will disappear when the radial wave energy is attenuated far from the source of the radial wave.

- Time-lagged wave source is more immune to the disturbance from external wave source, i.e., more resilient to retain its constructive-destructive superposition line.

References

[1] N. Khan, A. Kalair, N. Abas and A. Haider, "Review of ocean tidal, wave and thermal energy technologies", *Renewable Sustainable Energy Rev.*, Vol. 72, pp. 590-604, (2017).

[2] H. S. Kang, M. Q. H. Shaharuddin, K. Q. Lee, A. Steven, U. G. M. Arif, N. Khaliddin and S.L. Siow, "Numerical analysis of point absorber for wave energy conversion in Malaysian seas", *Progress Energy Environ.*, Vol. 1, pp. 25-39 (2017).

[3] N.V. Viet and Q. Wang, "Ocean wave energy pitching harvester with a frequency tuning

capability", *Energy*, Vol. 162, pp. 603-617 (2018).

[4] S. F. Nabavi, A. Farshidianfar and A. Afsharfard, "Novel piezoelectric-based ocean wave energy harvesting from offshore buoys", *Appl. Ocean Res.*, Vol. 76, pp. 174-183, (2018).

[5] Y. Hou, H. Yuan, X. Qu, H. Chen and L. Li, "Synthesis and high-performance electromagnetic wave absorption of SiC@C composites", *Mater. Lett.*, Vol. 209, pp. 90-93, (2017).

[6] C. Liang, W. Qin and Z. Wang, "Cobalt doping-induced strong electromagnetic wave absorption in SiC nanowires", *J. Alloys Compd.*, Vol. 781, pp. 93-100, (2019).

[7] J. Zhang, R. Shu, C. Guo, R. Sun, Y. Chen and J. Yuan, "Fabrication of nickel ferrite microspheres decorated multi-walled carbon nanotubes hybrid composites with enhanced electromagnetic wave absorption properties", *J. Alloys Compd.*, Vol. 784, pp. 422-430, (2019).

[8] S. Dong, X. Zhang, P. Hu, W. Zhang, J. Han and P. Hu, "Biomass-derived carbon and polypyrrole addition on SiC whiskers for enhancement of electromagnetic wave absorption", *Chem. Eng. J.*, Vol. 359, pp. 882-893, (2019).

[9] P. Liu, J. Jang, S. Yang and H. Sohn, "Fatigue crack detection using dual laser induced nonlinear ultrasonic modulation", *Opt. Lasers Eng.*, Vol. 110, pp. 420-430, (2018).

[10] L. Hua, B. Wang, X. Wang, X. He and S. Guan, "In-situ ultrasonic detection of resistance spot welding quality using embedded probe", *J. Mater. Process. Technol.*, Vol. 267, pp. 205-214.

[11] Y. Chen, G. Xie, J. Chang, J. Grundy and Q. Liu, "A study of coal aggregation by standing-wave ultrasound", *Fuel*, Vol 248, pp. 38-46, (2019).

[12] X. Luo, J. Cao, H. Yin, H. Yan and L. He, "Droplets banding characteristics of water-in-oil emulsion under ultrasonic standing waves", *Ultrasonic – Sonochemistry*, Vol. 41, pp. 319-326, (2018).

[13] X. Luo, H. Gong, J. Cao, H. Yin, Y. Yan and L. He, "Enhanced separation of water-in-oil emulsions using ultrasonic standing waves",

Chem. Eng. Sci., Vol. 209, pp. 285-292, (2019).

[14] H. Su-xia, L. Ji-jun, H. Bin, L. Ru-song and S. Tao, "The treatment of radioactive wastewater by ultrasonic standing wave method", *J. Hazard. Mater.*, Vol. 274, pp. 41-45, (2014).

[15] W.Y. Tey, K. M. Lee, N. A. C. Sidik and Y. Asako, "Delfim-Soares explicit time marching method for modelling of ultrasonic wave in microalgae pretreatment", *IOP Conf. Series: Earth Environ. Sci.*, Vol. 268, 012106, (2019).

[16] W.Y. Tey, H. Alehossien, Z. Qin, K. M. Lee, H. S. Kang and K. Q. Lee, "On stability of time marching in numerical solutions of rayleigh-plesset equation for ultrasonic cavitation", *Mater. Sci. Energy Technol.*, Vol. 463, 012117, (2020).

[17] H. Kang, G. Zhou and Q. Li, "Thermoacoustic effect of traveling-standing wave", *Cryogenics*, Vol. 50, No. 8, pp. 450-458, (2010).

[18] J. Callanan and M. Nuoh, "Optimal thermoacoustic energy extraction via temporal phase control and traveling wave generation", *Appl. Energy*, Vol. 241, pp. 599-612.

[19] D. J. Mead, "Free wave propagation in periodically supported, infinite beams", *J. Sound Vibr.*, Vol. 11, No. 2, pp. 181-197, (1970).

[20] J. Morsbøl and S. V. Sorokin, "Elastic wave propagation in curved flexible pipes", *Int. J. of Solis Struct.*, Vol. 75-76, pp. 143-155, (2015).

[21] A. M. Shafei and H. R. Shafei, "Dynamic behavior of flexible multiple links captured inside a closed space", *J. Comput. Non-linear Dyn.*, Vol. 11, No. 5, 051016, (2016).

[22] S. Chen, Y. Song and H. Zhang, "Wave propagation in L-shape beams with piezoelectric shunting arrays", *Shock Vib.*, Vol. 11, 051016, (2016).

[23] S. Klinaku and V. Berisha, "The Doppler effect and similar triangles", *Results Phys.*, Vol. 12, 846-852 (2019).

[24] W.Y. Tey, "Review on Klinaku-Berisha equation via numerical modelling for acoustical Doppler effect", *Appl. Acoust.*, Vol. 180, 108080 (2021).

[25] F. Nicassio, S. Carrino and G. Scarcelli, "Elastic waves interference for the analysis of

disbonds in single lap joints", *Mech. Syst. Signal Process*, Vol. 128, pp. 340-351, (2019).

[26] J. Yu, Q. Li and W. Ye, "Investigation of wave interference effect in Si/Ge superlattices with interfering Monte Carlo method", *Int. J. Heat Mass Transfer*, Vol. 128, pp. 270-278, (2019).

[27] J. M. Chern and S. N. Huang, "Study of nonlinear wave propagation theory. II. Interference phenomena of single-component dye adsorption waves", *Sep. Sci. Technol.*, Vol. 34, No. 10, pp. 1993-2011, (1999).

[28] J. Y. Lee and Y. X. Wong, "Polarization-standing-wave interferometer for displacement measurement", *Opt. Laser Technol.*, Vol. 111, pp. 110-114, (2019).

[29] P. Dou, T. Wu, Z. Luo, Z. Peng and T. Sarkodie-Gyan, "The application of the principle of wave superposition in ultrasonic measurement of lubricant film thickness", *Meas.*, Vol. 137, pp. 312-322, (2019).

[30] J. H. Lee, W. Y. Tey, K. M. Lee, H. S. Kang and K. Q. Lee, "Numerical simulation on ultrasonic caviatation due to superposition of acoustic waves", *Mater. Sci. Energy Technol.*, Vol. 3, pp. 593-600, (2020).

[31] J. C. Tannehill, D. A. Anderson and R. H. Pletcher, *Computational Fluid Mechanics and Heat Transfer*, 2nd ed., Taylor & Francis, pp. 102-103, (1997).

[32] T. Kajishima and K. Taira, *Computational Fluid Dynamics: Incompressible Turbulent Flows*, Springer International Publishing, pp. 51-54, (2017).

[33] D. C. Chang, "A quantum mechanical interpretation of gravitational redshift of electromagnetic wave", *Optik*, Vol. 174, pp. 636-641, (2018).

[34] U. Y. Ziya, "Wave diffraction by a perfect electromagnetic conductor wedge", *Optik*, Vol. 182, pp. 761-765, (2019).

[35] J. J. Arvydas, "Particles and quantum waves diffusion in physical vacuum", *Results Phys.*, Vol. 11, pp. 148-151, (2018).

[36] P. H. Chavanis, "Derivation of a generalized Schrödinger equation for dark matter halos from the theory of scale relativity", *Phys. Dark Universe*, Vol. 22, pp. 80-95, (2018).

[37] Frank Fahy, *Foundations of Engineering Acoustics*, Academic Press, (2000).

How to cite this paper: